LOCALIZATION AND LEVEL OF PROAPOPTOTIC PROTEIN REGULATORS IN A RAT LUNG TISSUE DURING DEVELOPMENT OF ACUTE EXPERIMENTAL BRONCHOPNEUMONIA

D. S. ZIABLITSEV[1]✉, A. O. TYKHOMYROV[2], O. O. DYADYK[3],
S. V. KOLESNIKOVA[1], S. V. ZIABLITSEV[1]

[1]Bogomolets National Medical University, Kyiv, Ukraine;
[2]Palladin Institute of Biochemistry, National Academy of Sciences of Ukraine, Kyiv;
[3]Shupyk National Healthcare University of Ukraine, Kyiv;
✉e-mail: denis898@ukr.net

Apoptosis plays an important role in the development of acute inflammatory lung injury (AILI) and its consequences, which can be realized in different cells with distinct intensity and rate. The aim of this study was to determine the distribution and expression intensity of apoptosis markers in the lungs of rats in the AILI model with endotracheal introduction of capron thread and LPS. Immunoblotting and immunohistochemical studies were performed using monoclonal antibodies against Bax and caspase-3 proteins. It was shown that Bax level increased significantly with the peak on the 7th day. The second peak of Bax 40 dimeric form was noted on the 21st day. The level of both pro-caspase-3 and active caspase-3 was also dramatically increased with a maximum on the 5th day and the second peak of active caspase-3 content was observed on the 21st day. These changes reflected the activation of apoptosis in key trigger periods of AILI during the development of exudative hemorrhagic pneumonia and subsequent fibrotic remodeling of the lungs.

K e y w o r d s: caspase-3, Bax, apoptosis, AILI, lipopolysaccharide.

Acute inflammatory lung injury (AILI) is a clinical syndrome that arises as a consequence of a wide range of pulmonary and extrapulmonary pathologies. Among them, acute respiratory distress syndrome (ARDS), which is often develops during coronavirus disease-19 (COVID-19), has attracted an essential attention in attempt to explore the main pathogenetic mechanisms underlying lung injury by SARS-CoV-2 [1, 2]. Already at its early stage, ARDS with hyperimmune diffuse exudative inflammation, destruction of alveoli, endothelial damage and the development of capillary leakage syndrome is formed [2]. At this stage, lethal outcome can occur due to acute respiratory failure, but in most cases the acute exudative stage becomes proliferative with the development of diffuse pulmonary fibrosis [3].

The main cause of death in patients with COVID-19 was the acute respiratory and pulmonary heart failure, multiorgan dysfunction [4]. The most pronounced changes in the lungs include multiple total bilateral lesions of the lower lobes with changes in the parenchyma and stroma, impaired microcirculation in the form of acute dyscirculatory and ischemic changes, coagulopathies. In patients who died of COVID-19-related respiratory failure, the histological picture in the lungs showed diffuse alveolar damage with lymphocytic infiltration, severe endothelial damage, widespread thrombosis, and microangiopathy [5].

Apoptosis plays an important role in the development of AILI and its consequences, which accompanies all stages of the pathological process, but can be realized in different cells with different intensity and rate [6]. For example, apoptosis of polymorphonuclear leukocytes in the lungs prevents inflammation and the development of ARDS, while Fas/FasL-mediated apoptosis of alveolar epithelial cells contributes to acute lung damage and pulmonary fibrosis; apoptosis of pulmonary epithelial and endothelial cells promotes the development of emphysema. Apoptosis is activated in response to various types of lung damage, such as trauma, septic shock, pneumonia, and is mediated by neutrophils and macrophages that accumulated at the site of injury and inflammation [7]. Activation of apopto-

sis in AILI plays a crucial role in the development of acute lung disease and related disorders such as AVHD and fibrosis. Modulation of the apoptosis development is considered as a promising area for the correction of lung injuries induced by various factors [8].

Induced pneumonia in wild-type mice has been described to be accompanied by significant activation of caspase-3, which is a key enzyme in triggering apoptotic signal [9]. Due to the accumulation of chemokines, this mechanism promotes the involvement of macrophages in the site of inflammation. Activation of caspase-3 and increased mitochondrial apoptosis have been shown in bacterial lung disease (*Streptococcus pneumoniae*) [8]. Transforming growth factor-β1 (TGF-β1) is known to induce pulmonary inflammation, fibrosis, myofibroblast accumulation, and alveolar destruction mediated by apoptosis and caspase-3 activation [10].

The aim of this study was investigate the features of tissue distribution of apoptosis markers and the intensity of their expression in the lungs in the AILI model with endotracheal introduction of polyamide thread and LPS solution.

Materials and Methods

Experiments. AILI was reproduced by endotracheal injection of a foreign body (polyamide thread), which allows obtaining a slow development of the inflammatory process with the development of diffuse fibrosis of the lung parenchyma after four weeks [11]. To exacerbate the pathological process, in addition to the introduction of polyamide thread, the animals were systemically and endotracheally injected with LPS solution.

To do this, intact Wistar rats ($n = 50$) weighing 180-190 g for one and two days before AILI modeling intraperitoneally administered a solution of LPS (*Salmonella typhi* lipopolysaccharide, Pyrogenal) at a dose of 250 mg/kg. A sterile polyamide thread 2.5 cm long and 0.2 mm thick was inserted into the needle to a depth of 2.5 cm, after which 50 μl of LPS solution (12.5 mg/kg) was injected into the trachea.

The work was guided by the norms and principles of EU Directive 2010/63 on the protection of animals, the Declaration of Helsinki (2008) and the requirements of the Law of Ukraine "On Protection of Animals from Cruelty" (No 1759-VI of 15.12.2009). The animals were kept in an animal house on a standard diet.

The introduction of polyamide thread and LPS solution was accompanied by several convulsive inhalations and exhalations, intense respiration. In 10-15 minutes at auscultation growing damp rales were listened. Breathing became difficult, with the involvement of the chest muscles, cyanosis increased, distant wet rales were heard, breathing was frequent, spastic. On the 1st day, the animals had severe wheezing, on the 3rd day, the symptom of pulmonary crepitation was clearly heard, severe cyanosis was noted. After the 5th day, the condition of the animals was stabilized, wet rales disappeared, breathing became hard, intermittent. Mortality during the experiment was 36%. In this study, the animals were observed for 21 days.

Immunoblotting. In the next series of experiments on the 1st, 3rd, 5th, 7th, 14th and 21st day of observation, experimental animals with introduction of polyamide thread and LPS solution ($n = 5$ per each day of observation, total – 30) were terminated from the experiment under thiopental anesthesia.

The thoracic cavity was dissected, the lungs were separated. Determination of the level of Bax proteins and caspase-3 in lysates of lung tissue was performed by immunoblotting. Lung tissue samples were frozen and crushed in a liquid nitrogen, ground and homogenized in 50 mM Tris-HCl buffer (pH 7.4) with the addition of phosphatase and protease inhibitors (Pierce Protease and Phosphatase inhibitor, ThermoScientific, USA, # A32961) and centrifuged at 16,000 g for 60 min at 4°C. After centrifugation, the concentration of total protein in supernatants was measured spectrophotometrically [12]. Electrophoresis was performed in 8% polyacrylamide gel with sodium dodecyl sulfate (SDS-PAGE) [13] in a vertical gel electrophoresis chamber (BioRad, USA). Concentration of the samples was performed at a voltage of 30 V, separation – 50 V. Proteins were transferred from the gel onto nitrocellulose membrane by electroblotting using a buffer solution containing 0.025 M Tris-HCl, 0.192 M glycine, and 25% methanol [14]. Membranes were blocked in a 5% solution of skimmed milk powder in buffered saline (PBS), then incubated with monoclonal antibodies to Bax protein and caspase-3 (ThermoFisher Scietific, USA). Rabbit anti-actin antibodies (Abcam, USA, cat. 20ab20272) were used to detect actin as a control of protein loading. After incubation with the primary antibodies, the membranes were washed in PBS, containing 0.05% Triton X-100 (PBST), and probed

with anti-species secondary antibodies conjugated with horseradish peroxidase. Immunoreactive bands were visualized by enhanced chemiluminescence (ECL) followed by autoradiography on X-ray films [18]. Semi-quantitative analysis was performed densitometrically using TotalLab software (TL120, Nonlinear Inc, USA). The molecular weights of proteins in the samples were determined by comparing their migration with the location of colored markers RulerTM Plus Prestained Protein Ladder (Thermo-Scientific, Lithuania, cat. № 26619, 10-230 kDa). The results of immunoblot analysis of both Bax and caspase-3 levels were calculated as values of correspondent immunoreactive band densities normalized to the actin level and expressed as % from the control values.

Immunohistochemical study. Specimens of tissue from different lung areas were fixed in a 10% solution of neutral buffered formalin (pH 7.4) for 24-36 h. After fixing in formalin, fragments of tissue were embedded into paraffin. Serial histological sections 2-3 μm thick were made from paraffin blocks on a rotary microtome NM 325 (Thermo Shandon, England). Immunohistochemical study was performed using monoclonal antibodies against caspase-3 (Caspase 3 Monoclonal Antibody, clone74T2; ThermoFisher Scietific, USA). Sections were placed on Super Frost Plus adhesive slides (Menzel, Germany). Citrate buffer (pH 6.0) was used for antigen retrival by boiling the samples for 5 min. Then, the detection system UltraVision Quanto HRP, chromogen dimethylaminobenzene Quanto, manufactured by Thermo Fisher Scientific (USA) was used for immunostaining. Sections were additionally counterstained with hematoxylin.

Microscopic examination and photo archiving were carried out using light-optical microscopes Axio Imager.A2 (Carl Zeiss, Germany) with a data processing system at the magnification of ×5, ×10, ×20, ×40 lenses, a 1.5 binocular attachment and 10 eyepieces with an ERc 5s camera, PrimoStar (Carl Zeiss, Germany) with a camera Axio Cam105.

The control group for immunoblotting and immunohistochemical study included 15 sham-operated animals ($n = 3$ per each day of observation).

Statistical procedures. Statistica 10 software (StatSoft, Inc., USA) was used for statistical analysis. Descriptive statistics were performed with the calculation of means (M) and their standard deviations (SD). Sample averages were compared using one-way analysis of variance (ANOVA), and values of $P < 0.05$ were considered statistically significant.

Results and Discussion

According to the results of immunoblot densitometry analysis, the amount of Bax 40 protein in the lung tissue significantly exceeded the control values during the entire observation period (Fig. 1). The maximum increase was observed on the 7th day, when its content exceeded the control by 26.6 times ($P < 0.001$). The second peak of increase in protein content was observed on the 21st day (by 22.5 folds; $P < 0.001$).

Relatively weak immunostaining of 20 kDa Bax monomeric form was observed in the samples throughout all experimental period (Fig. 1, *A*). This observation is either due to the intense formation of dimeric Bax form or specific binding of the used antibody, which could preferentially recognize 40 kDa Bax polypeptide. During the observation, the Bax protein content, reached the peak value on the 7th day (17.2 times; $P = 0.0015$).

Immunoblotting analysis of caspase-3 level showed a significant up-regulation of both forms of the enzyme (pro-caspase-3 and cleaved, or active caspase-3) in the control (Fig. 2). The two-phase dynamics of enzyme content in tissue with the peaks on the 5th and 21st days of observation was determined. The content of pro-caspase-3 on the 5th day was increased by 3.1 folds ($P < 0.001$), then decreased to the control values, and on the 21st day increased again by 2.4 folds compared to control ($P < 0.001$). Similarly, the content of active caspase-3 on the 5th day was increased by 8.9 folds ($P = 0.0012$), and on the 21st day – by 11.0 folds ($P < 0.001$).

Immunohistochemical staining of caspase-3 revealed certain features of the tissue distribution of this enzyme (Fig. 3), which was in agreement with the dynamics of its content showed by immunoblotting. In the control group, there was a relatively small number of immunopositive cells in the interstitium (up to 15-20%), which could be identified as macrophages and fibroblasts by morphological characteristics. It is worth-noting that single alveolocytes were also positively stained.

After the 1st day, the intensity of the immunostaining increased significantly, the number of immunopositive cells of the interstitium increased to 50%. Macrophages were large, found not only in lung tissue but also in the lumen of the alveoli. Almost all alveolocytes line the alveolar ducts and alveoli had immunopositive staining. In the lung parenchyma, there are foci of emphysematically dilated
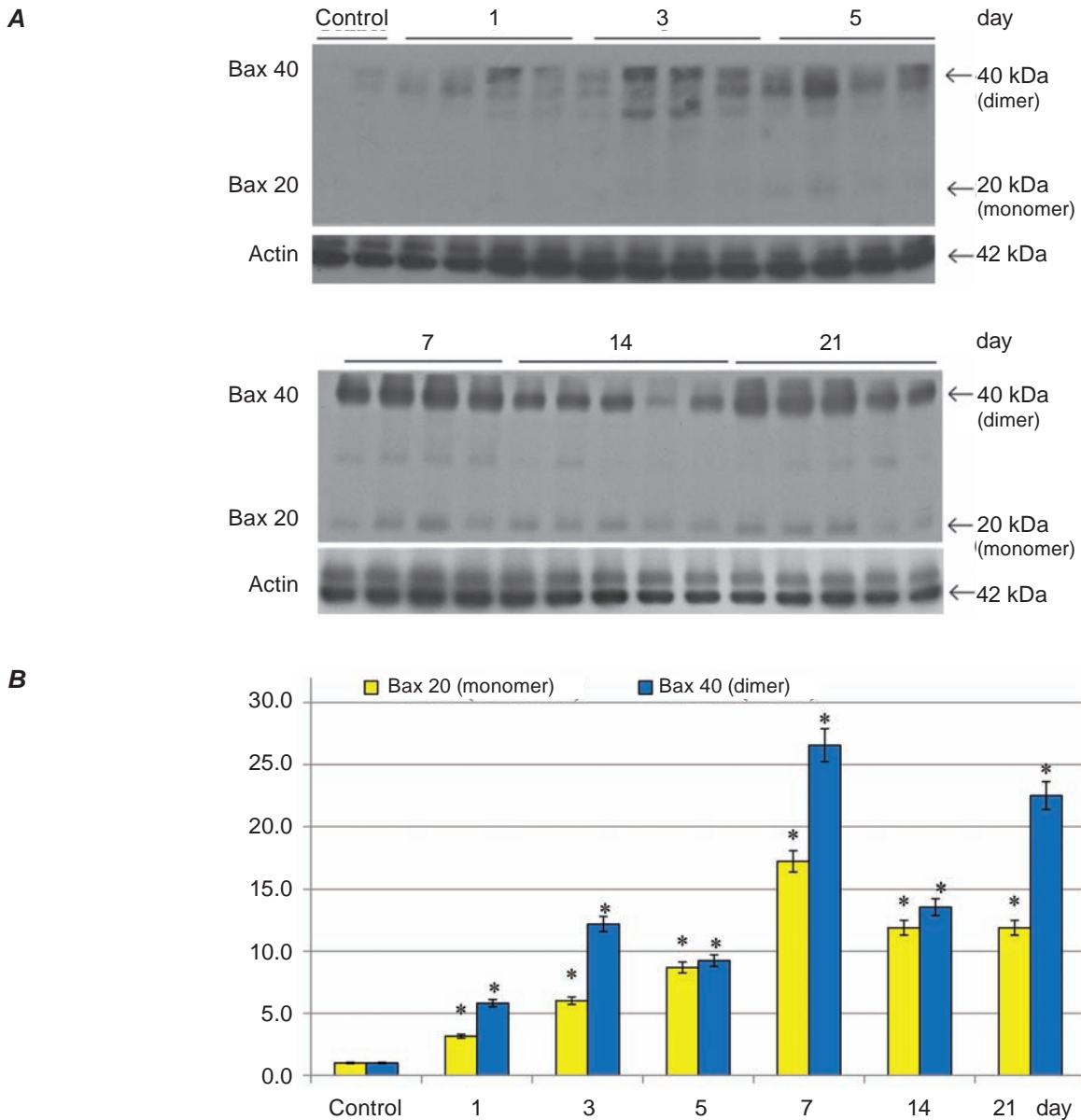
*Fig. 1. The level of Bax 20 and Bax 40 proteins in rat lung tissue during experimental pneumonia; **A** – representative blotograms of Bax proteins; **B** – results of densitometry analysis of blotograms. *The difference is statistically significant compared with the control value ($P < 0.05$)*

alveoli with thinning and ruptures of the interalveolar septa.

The morphological characteristics on the 3rd and 5th day of observation were similar: against the background of common foci of atelectasis and severe parenchymal edema, a large number of immunopositive cells in the interstitium and on the inner surface of the alveoli were observed. Serous-hemorrhagic exudate with leukocyte impurities, I and II types epitheliocyte hyperplasia were noted in the alveoli.

On the 7th day, the total intensity of immunohistochemical staining and the number of immunopositive cells were reduced compared to previous dates. In the interalveolar septa, there are signs of high fibroblastic activity with the appearance of fibrillar network, which indicate the development of diffuse fibrosis. Serous-hemorrhagic exudate with fibrin threads and neutrophil admixture was found in the alveoli.
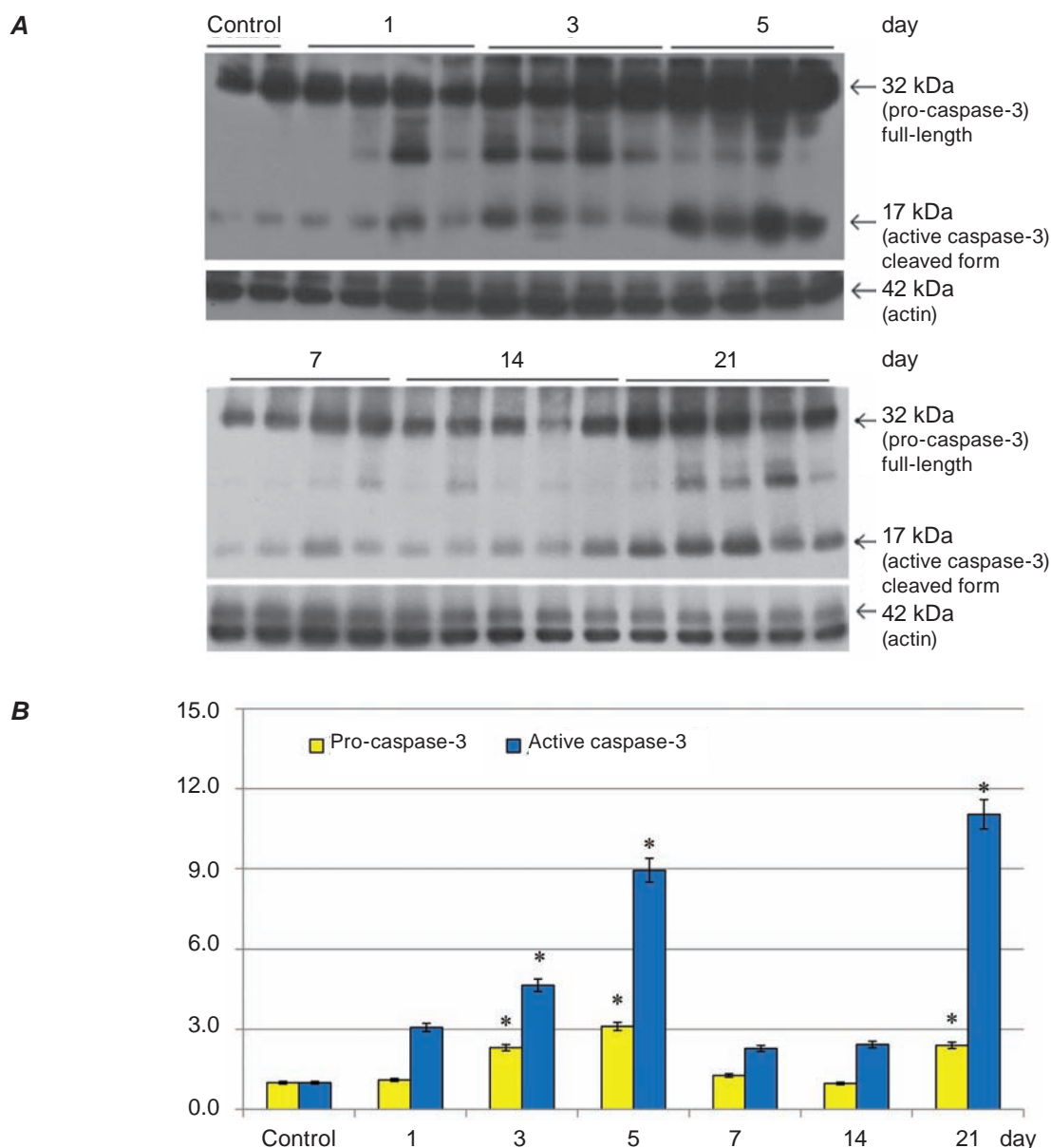
*Fig. 2. The level of pro-caspase-3 and active caspase-3 in rat lung tissue during experimental pneumonia; **A** – representative blotograms of caspase-3 proteins; **B** – results of densitometry analysis of blotograms. *The difference is statistically significant compared with the control value (P < 0.05)*

On the 14th day, with the common fields of chronic productive inflammation in the lung parenchyma, there was a repeated increase in the intensity of immunospecific staining; in the parenchyma large immunopositive macrophages was found; the number of fibroblasts increased, among them single cells had immunopositive staining. In the lungs, there are numerous areas of dense fibrosis (carnification), vessels of medium and small caliber with fibrosis, in some places with complete obliteration of the lumen.

On the 21st day, the overall intensity of immunospecific staining was significantly increased, there are granulomas in the interstitium with an accumulation of macrophages, 50% of them had immunopositive staining. Most parenchymal fibroblasts were not caspase-3-positively stained.

Changes in the intensity of immunospecific staining of the bronchial epithelium (Fig. 4) were similar to such parenchymal cells, but had some peculiarities.
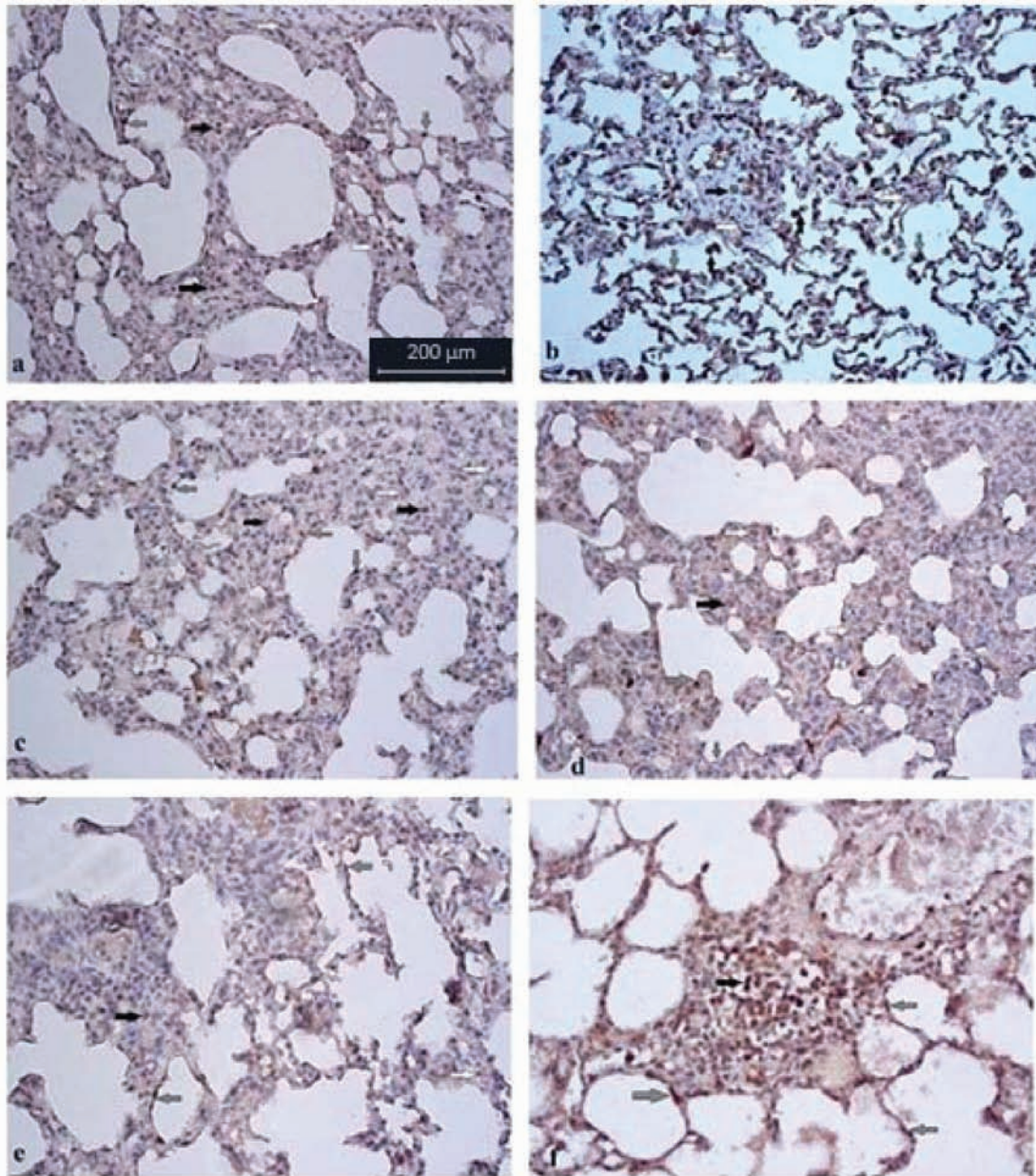
*Fig. 3. Microphotographs of the lung tissue of rats with an experimental bronchopneumonia. Representative results of immunohistochemical staining of caspase-3; black arrows indicate macrophages, white – fibroblasts, grey – alveolocytes; magnification ×200; **a** – control group; small number (15-20%) of immunopositive macrophages and fibroblasts in the interstitium of interalveolar septa, single immunopositive alveolocytes II type; **b** – 1ˢᵗ day; up to 50% of interstitial cells have immunopositive staining, among which large macrophages and regrown fibroblasts are clearly visualized; a small number of immunopositive macrophages are found in the lumen of the alveoli; almost all alveolocytes I and II types have immunopositive staining; **c** – 5ᵗʰ day; a large number of immunopositive cells in the interstitium and on the inner surface of the alveoli; severe edema of the interalveolar septa, areas of emphysema; **d** – 7ᵗʰ day; the intensity of staining and the number of immunopositive cells in the visual comparison with previous terms is reduced; areas of atelectasis are found along with emphysematous areas; **e** – 14ᵗʰ day; a large number of large immunopositive macrophages; single immunopositive fibroblasts and alveolocytes; widespread parenchymal fibrosis; **f** – 21ˢᵗ day; accumulation of macrophages in the interstitium, 50% of macrophages have immunopositive staining; most fibroblasts are not immunopositevely stained; single immunopositive alveolocytes, mainly II type; positive staining in the vascular endothelium; collagenosis of the vascular wall*
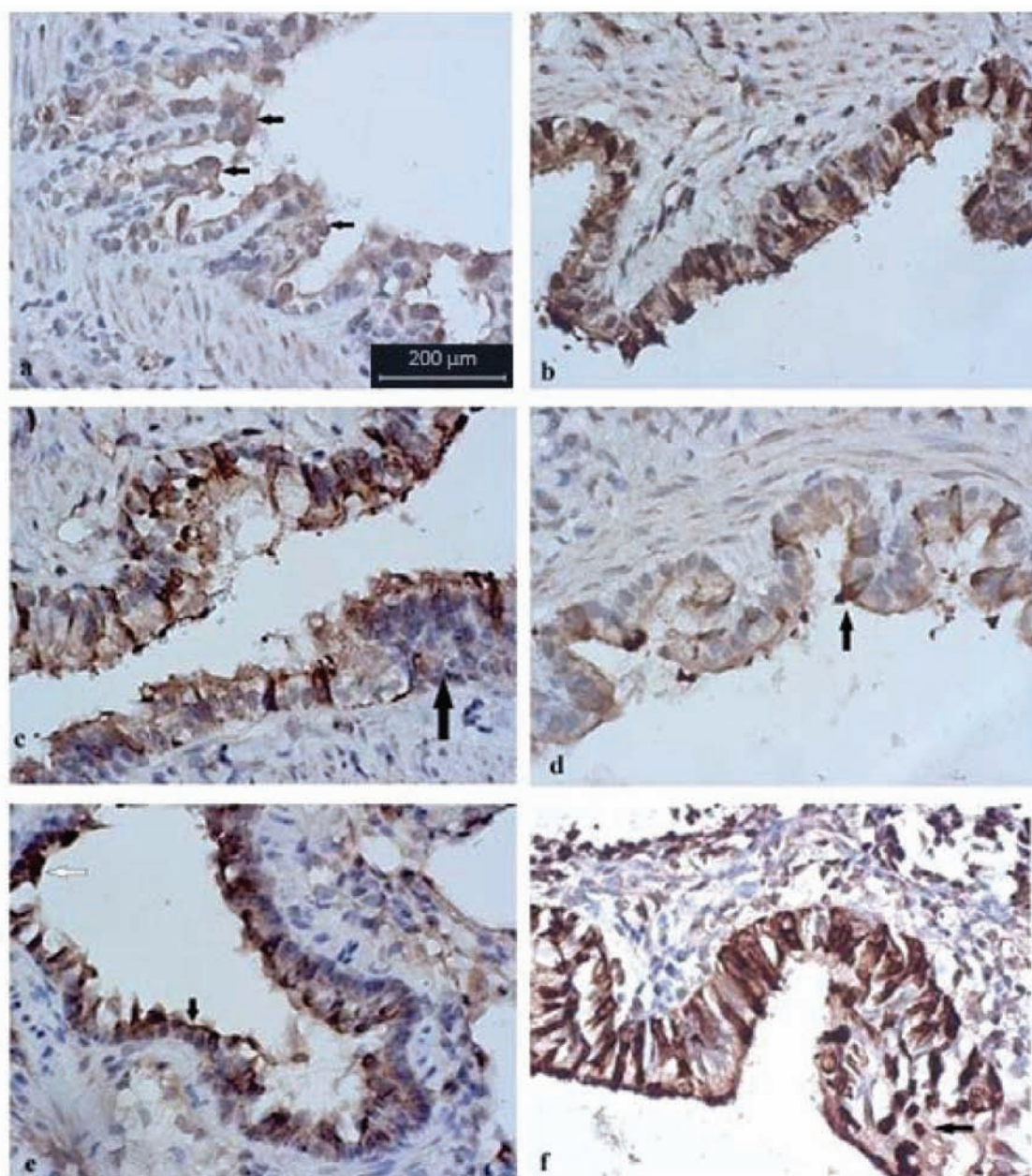
*Fig. 4. Microphotographs of the lung tissue of rats with an experimental bronchopneumonia. Representative results of immunohistochemical staining on caspase-3 in bronchial wall; magnification ×400; **a** – control group; immunopositive staining is expressed in exfoliating epithelial cells (arrows); **b** – 1st day; almost all epithelial cells have intense immunopositive staining; **c** – 5th day; bronchial epithelial hyperplasia (arrow), newly formed cells do not contain specific staining; **d** – 7th day; single epithelial cells express an immunospecific staining of low intensity (arrow); **e** – 14th day; intense staining of the apical surface of the bronchial epithelium (black arrow); intense staining of degenerating cells (white arrow); **f** – 21st day; intense staining of almost all columnar epithelial cells; intense staining of degenerated cells (arrow)*

In the control group, low-intensity immunopositive staining was observed only in exfoliated epithelial cells. This result was sharply contrasted with a significant increase in the intensity of staining after the 1st day, when almost all epithelial cells display intense immunopositive staining localized throughout the cytoplasm, which could be considered as a sign of cell degeneration. The mucous membrane of the bronchi and bronchioles showed signs of hypersecretory activity due to hyperplasia of the ciliary

epithelium and goblet cells with parenchymal dystrophy, foci of desquamation and exudate in the lumen. These changes had a tendency to aggravation in time. On the 3-5th day, hyperplasia of the bronchial epithelium was noted; the newly formed epithelial cells was not stained immunopositively.

On the 7th day, the total intensity of bronchial epithelial staining was reduced and only single epithelial cells had weak immunospecific staining. On the 14th day, the second wave of elevation in immunopositive staining the intensity of the cytoplasm of bronchial epithelial cells was observed. Cellular apical surface was intensively stained, as well as cells that were in the stage of degeneration and exfoliation. On the 21st day, immunopositive staining was further increased, and immunostaining in the epithelial cells was seen as intensely colored columns. In some cases there were proliferating cells with signs of degeneration.

Thus, it was found that the applied AILI model leads to the development of acute exudative-hemorrhagic inflammatory process in the lungs. Already in the first hour after the kapron thread and LPS introduction hyperimmune inflammation was formed with the development of ARDS. Subsequently, damage to the vessels of the microcirculatory tract, lung parenchyma in the form of emphysema with ruptures of the interalveolar septa with their pronounced leukocyte infiltration and the development of hemorrhagic pneumonia on the 3rd day. At the same time, from the 5th to the 7th day, reactive hyperplasia of lymphoid follicles, active fibrosis of the bronchi and lung parenchyma, hyalinosis of the vessels were noted. On the 14th day there were signs of chronic productive inflammation with the development of diffuse pulmonary fibrosis and vascular sclerosis on the 21st day.

Comparison of such data with the results of immunoblotting analysis, allowed to analyze some pathological mechanisms of these phenomena. The content of Bax proteins in acute pneumonia increased significantly with a peak on the 7th day. For the dimeric form Bax 40, the second peak of the increase in tissue content was noted – on the 21st day. Multidomain proapoptotic proteins of the Bax family have constitutive expression and are activated under the conditions of accumulation of intracellular damage with the formation of a monomeric form [6, 7]. The latter destabilize the mitochondrial membrane with the release of cytochrome C. In the control group, the content of Bax 20 monomer in lung tissue was at almost zero (see Fig. 1, *A*), a relatively small increase in this form of protein was observed in the samples on the 1st day, while later (3-7th day) the content of Bax 20 increased significantly, which, in our opinion, was due to increasing tissue damage and development of hemorrhagic pneumonia. The consistently high protein content observed on days 14-21 may have been associated with active remodling of the lung parenchyma during this period and the development of diffuse fibrosis.

The content of both forms of caspase-3 (procaspase-3 and active caspase-3) also increased many times with a maximum increase on the 5th day, while split caspase-3 gave the second peak of tissue content – on the 21st day. The cleaved form of caspase-3 is an effector enzyme that makes the cell on the apoptosis path [6, 7]. Its significant activation on days 3-5 and 21 confirmed the activation of apoptosis in these periods, which was associated with widespread tissue damage in the development of hemorrhagic pneumonia and fibrous lung remodeling in the future.

Apoptotic damage to alveolar epitheliocytes and remodeling with persistent fibroblast proliferation has been shown to be critical to the terminal stage of fibrosis [15]. However, the degree of fibrosis was associated with the activation of caspase-3 in the cytoplasm of epithelial cells.

The results obtained in this study were completely consistent with those obtained in similar experimental studies [16, 17]. It was shown that intratracheal administration of LPS (5 mg/kg) to rats after 24 h led to the accumulation of large numbers of neutrophils in the intra- and interalveolar space, thickening of the alveolar wall due to edema, increased of myeloperoxidase activity, lipid peroxidation and caspase-3 activity [16]. Bax proapoptotic protein expression and lung cell apoptosis also increased.

12 hours after intraperitoneal administration of LPS (40 mg/kg) in the blood of wild-type mice significantly increased levels of interleukin-18, in the lungs appeared pronounced neutrophilic infiltration and increased activity of myeloperoxidase and caspase-3 on the background of significant interalveolar edema, increased apoptosis [17]. According to the authors, endogenous interleukin-18, formed by LPS, induces the expression of intercellular adhesion molecules (ICAM-1), which recruits neutrophils and inhibits their apoptosis with increased oxidative damage to lung tissue, leading to edema.

The dynamics of immunohistochemical staining activity of caspase-3 fully corresponded to its content according to the immunoblotting study, but allowed to establish certain features of the tissue distribution of the enzyme. On the 1st day, activated macrophages and fibroblasts had the greatest activity of caspase-3, as well as bronchial epitheliocytes, which had a pronounced immunospecific color of the cytoplasm against the background of hyperplasia and desquamation. Subsequently, against the background of severe parenchymal edema, the number of immunopositive cells in the interalveolar septa increased, while in the bronchial mucosa there were signs of severe hyperplasia with no immunopositive staining. On the 7th day, the content and activity of caspase-3 in both the lungs and the bronchial epithelium decreased significantly with a subsequent re-increase on the 21st day.

In the development of experimental silicosis in rats caspase-3 played a leading role due to the activation of apoptosis [18]. It was noted that caspase-3 was expressed in alveolar epithelial cells, pulmonary macrophages and infiltrated inflammatory cells. This is the localization of immunospecific staining was observed in our study.

Experimental blunt trauma to the chest with pulmonary contusion led to acute pneumonia and significantly increased the activity of caspases, including caspase-3, which was accompanied by apoptosis of alveolocytes II type [19]. The latter showed both signs of reactive hyperplasia and active immunospecific staining throughout the observation.

In the lungs, acute inflammatory reactions are initiated by granulocytes (neutrophils or eosinophils), which respond rapidly to harmful respiratory stimuli [20]. Importantly, the result of AILI is regulated by the balance between pro- and anti-inflammatory regulators, among which the interaction of granulocytes, macrophages and epithelial cells is of major importance [21]. At the same time, apoptosis of neutrophils/eosinophils and their removal by macrophages with cessation of leukocyte infiltration and restoration of normal vascular permeability should be activated in a timely manner. LPS-induced reactivation of proinflammatory reactions with the development of hyperimmune inflammation, respiratory failure and high mortality took place in the applied model. The activity of apoptotic proteins increased in two phases with maxima on days 5-7 and 14-21, which reflected the key trigger points of AILI – the development of exudative-hemorrhagic pneumonia and diffuse pulmonary fibrosis.

The analysis of the obtained data suggested that there are certain parallels in the development of LPS-induced experimental aspiration pneumonia, which was modeled in this study, with acute lung damage induced by SARS-CoV-2 invasion. This suggestion is also confirmed by the recently reported data on the significant activation of caspase-3 under the action of the S1-subunit of SARS-CoV-2 on the vascular endothelium in COVID-19 [22]. Our study also found positive caspase-3 endothelial staining in AILI. This allowed us to consider that vascular endothelial apoptosis is not a specific result of the S1-subunit of SARS-CoV2, but rather a general pattern of inflammation in AILI.

Conclusions. This study shows the features of tissue distribution and dynamics of the content of proapoptotic proteins Bax and caspase-3 in acute experimental bronchopneumonia. The applied experimental model of AILI led to the development of an acute exudative-hemorrhagic inflammatory process in the lungs with the output of diffuse fibrosis. The changes in the levels and histological distribution of the key pro-apoptotic regulators, Bax and caspase-3, indicate the activation of apoptosis during the crucial periods of AILI development to trigger general tissue injury as a sign of a hemorrhagic pneumonia and further step of fibrous lung tissue remodeling.

ЛОКАЛІЗАЦІЯ ТА ВМІСТ ПРОАПОПТОТИЧНИХ РЕГУЛЯТОРНИХ ПРОТЕЇНІВ У ТКАНИНІ ЛЕГЕНЬ ЩУРІВ ЗА РОЗВИТКУ ГОСТРОЇ ЕКСПЕРИМЕНТАЛЬНОЇ БРОНХОПНЕВМОНІЇ

Д. С. Зябліцев[1✉], А. О. Тихомиров[2],
О. О. Дядик[3], С. В. Колесникова[1],
С. В. Зябліцев[1]

[1]Національний медичний університет
імені О. О. Богомольця, Київ, Україна;
[2]Інститут біохімії ім. О. В. Палладіна
НАН України, Київ;
[3]Національний університет охорони здоров'я
України імені П. Л. Шупика, Київ;
✉e-mail: denis898@ukr.net

Апоптоз відіграє важливу роль у розвитку гострого запального ураження легень (AILI) та його наслідків, які можуть реалізовуватися в різних клітинах із різною інтенсивністю та швидкістю. Мета цього дослідження полягала у визначенні розподілу та інтенсивності експресії маркерів апоптозу в легенях щурів із моделлю AILI з ендотрахеальним введенням капронової нитки та LPS. Імуноблотингові та імуногістохімічні дослідження проводили з використанням моноклональних антитіл проти протеїнів Bax і каспази-3. Показано, що рівень Bax значно підвищувався з піком на 7-й день. Другий пік димерної форми Bax 40 було відзначено на 21-й день. Рівні як прокаспази-3, так і активної каспази-3 також різко підвищувалися з максимумом на 5-у добу, а другий пік вмісту активної каспази-3 спостерігався на 21-у добу. Ці зміни відображали активацію апоптозу в ключові тригерні періоди AILI під час розвитку ексудативної геморагічної пневмонії і подальшого фіброзного ремоделювання легень.

К л ю ч о в і   с л о в а: каспаза-3, Bax, апоптоз, AILI, ліпополісахарид..

References

1. World Health Organization. Coronavirus disease (COVID-19) pandemic. Available et https://www.who.int/emergencies/diseases/novel-coronavirus-2019 (accessed, July, 2022).

2. Cai A, McClafferty B, Benson J, Ramgobin D, Kalayanamitra R, Shahid Z, Groff A, Aggarwal CS, Patel R, Polimera H, Vunnam R, Golamari R, Sahu N, Bhatt D, Jain R. COVID-19: Catastrophic Cause of Acute Lung Injury. *S D Med.* 2020; 73(6): 252-260.

3. Suster S, Moran AC. Biopsy interpretation of the lung. 1st ed. Lippincott Williams & Wilkins, Wolters Kluwer; 2013. 417 p.

4. Rybakova MG, Karev VE, Kuznetsova IA. Anatomical pathology of novel coronavirus (COVID-19) infection. First impressions. *Arkh Patol.* 2020; 82(5): 5-15. (In Russian).

5. Ackermann M, Verleden SE, Kuehnel M, Haverich A, Welte T, Laenger F, Vanstapel A, Werlein C, Stark H, Tzankov A, Li WW, Li VW, Mentzer SJ, Jonigk D. Pulmonary Vascular Endothelialitis, Thrombosis, and Angiogenesis in Covid-19. *N Engl J Med.* 2020; 383(2): 120-128.

6. Lu Q, Harrington EO, Rounds S. Apoptosis and lung injury. *Keio J Med.* 2005; 54(4): 184-189.

7. Chopra M, Reuben JS, Sharma AC. Acute lung injury:apoptosis and signaling mechanisms. *Exp Biol Med (Maywood).* 2009; 234(4): 361-371.

8. N'Guessan PD, Schmeck B, Ayim A, Hocke AC, Brell B, Hammerschmidt S, Rosseau S, Suttorp N, Hippenstiel S. Streptococcus pneumoniae R6x induced p38 MAPK and JNK-mediated caspase-dependent apoptosis in human endothelial cells. *Thromb Haemost.* 2005; 94(2): 295-303.

9. Neff TA, Guo RF, Neff SB, Sarma JV, Speyer CL, Gao H, Bernacki KD, Huber-Lang M, McGuire S, Hoesel LM, Riedemann NC, Beck-Schimmer B, Zetoune FS, Ward PA. Relationship of acute lung inflammatory injury to Fas/FasL system. *Am J Pathol.* 2005; 166(3): 685-694.

10. Yamasaki M, Kang HR, Homer RJ, Chapoval SP, Cho SJ, Lee BJ, Elias JA, Lee CG. P21 regulates TGF-beta1-induced pulmonary responses via a TNF-alpha-signaling pathway. *Am J Respir Cell Mol Biol.* 2008; 38(3): 346-353.

11. Zyablitsev SV, Penskyy PYu, Litvinets ML, Kovalova AV, Salamaha AA. Dynamics of morphological manifestations of the experimental acute aspiration bronchopneumonia development. *Morphologia.* 2021; 15(1): 48-59.

12. Stoscheck CM. Quantitation of protein. *Methods Enzymol.* 1990; 182: 50-68.

13. Laemmli UK. Cleavage of structural proteins during the assembly of the head of bacteriophage T4. *Nature.* 1970; 227(5259): 680-685.

14. Towbin H, Staehelin T, Gordon J. Electrophoretic transfer of proteins from polyacrylamide gels to nitrocellulose sheets: procedure and some applications. *Proc Natl Acad Sci USA*. 1979; 76(9): 4350-4354.

15. Kuwano K, Hagimoto N, Maeyama T, Fujita M, Yoshimi M, Inoshima I, Nakashima N, Hamada N, Watanabe K, Hara N. Mitochondria-mediated apoptosis of lung epithelial cells in idiopathic interstitial pneumonias. *Lab Invest*. 2002; 82(12): 1695-1706.

16. Li T , Liu Y, Li G, Wang X, Zeng Z, Cai S, Li F, Chen Z. Polydatin attenuates ipopolysaccharide-induced acute lung injury in rats. I*nt J Clin Exp Pathol*. 2014; 7(12): 8401-8410.

17. Takahara M, Aoyama-Ishikawa M, Shuno K, Yamauhi C, Miyoshi M, Maeshige N, Usami M, Yamada T, Osako T, Nakao A, Kotani J. Role of endogenous IL-18 in the lung during endotoxin-induced systemic inflammation. *Acute Med Surg*. 2013; 1(1): 23-30.

18. Li X, Yan YH, Feng DY. Apoptosis and caspase-3 in the model of rat silicosis. *Zhong Nan Da Xue Xue Bao Yi Xue Ban*. 2005; 30(4): 441-443.

19. Seitz DH, Perl M, Mangold S, Neddermann A, Braumüller ST, Zhou S, Bachem MG, Huber-Lang MS, Knöferl MW. Pulmonary contusion induces alveolar type 2 epithelial cell apoptosis: role of alveolar macrophages and neutrophils. *Shock*. 2008; 30(5): 537-544.

20. Robb CT, Regan KH, Dorward DA, Rossi AG. Key mechanisms governing resolution of lung inflammation. *Semin Immunopathol*. 2016; 38(4): 425-448.

21. Belchamber KBR, Hughes MJ, Spittle DA, Walker EM, Sapey E. New Pharmacological Tools to Target Leukocyte Trafficking in Lung Disease. Front Immunol. 2021; 12: 704173.

22. Nuovo GJ, Magro C, Shaffer T, Awad H, Suster D, Mikhail S, He B, Michaille JJ, Liechty B, Tili E. Endothelial cell damage is the central part of COVID-19 and a mouse model induced by injection of the S1 subunit of the spike protein. *Ann Diagn Pathol*. 2021; 51: 151682.